Strength of Polystyrene–Poly(methyl methacrylate) Interfaces

K. L. Foster and R. P. Wool*

Department of Materials Science and Engineering, University of Illinois, 1304 West Green Street, Urbana, Illinois 61801

Received November 15, 1989; Revised Manuscript Received September 7, 1990

ABSTRACT: The fracture strength of polystyrene (PS) and poly(methyl methacrylate) (PMMA) interfaces was measured as a function of welding temperatures with a wedge cleavage fracture geometry. The fracture strength of 42.5 ± 4.5 J/m^2 is independent of the welding temperature in the range from 120 to 150 °C. This behavior agrees with a simple scaling argument in combination with Helfand's thermodynamic theory of incompatible mixing. Calculations of the equilibrium interpenetration depth (d_∞) of the incompatible interface using short-time welding data of symmetric interfaces yield a value with the same order of magnitude as determined by neutron reflection experiments of Higgins et al. and Russel et al. We calculate 60 ± 20 Å for a short-time welding case in comparison to Higgins' 25-Å result and Russel's 50-Å result. Helfand's theory predicts 27 Å for a PS–PMMA interface. Finally, on the basis of optical and X-ray photoelectron spectroscopy surface analysis of fractured PS–PMMA surfaces, less than 30% coverage of PS was on the PMMA side, indicating some cohesive fracture of PS, but no PMMA was transferred to the PS side. This occurred regardless of whether crazed or clear fracture areas were examined. An optical dye study supported this result, with as much as 20% of the PMMA crazed fracture surfaces testing positive for PS when high concentrations of the dye were used. Unlike the XPS study, PS was not observed on clear PMMA fracture surfaces. This may be due to optical intensity detection limits. We conclude that there is probably a combination of adhesive and cohesive failure, as has been reported.[6]

Introduction

The development of the strength of polymer interfaces is of interest to those studying both the motion of polymer molecules and the melt processing of homopolymers, block copolymers, and polymer blends. The evolution of strength is the result of macromolecular diffusion at an interface, which for the case of chemically identical species (symmetric amorphous case) results in the eventual disappearance of the interface with a fracture strength equal to that of a virgin sample.[1] A diffused chain from one side entangles with other chains across the interface, which, during fracture, is strained until it can either disentangle or fracture, depending on the rate and temperature of fracture. The relationship between the structure and strength of interfaces has recently been reviewed.[2]

This work studies the development of strength of the interface between two chemically incompatible amorphous polymers, polystyrene (PS) and poly(methyl methacrylate) (PMMA). As in the symmetric case, we believe the strength development is due to interpenetration of the polymer chains across the interface, leading to some degree of entanglement. But, because the polymers are incompatible, there is little mixing and thus almost no diffusion of the polymer chains. The interface does not disappear and the strength of the interface is constant after a short equilibrium welding time. Understandably, the strength of these interfaces is low in comparison with the symmetric systems.

In order to better understand the strength development process of the incompatible interface, we have examined the strength of a PS and PMMA interface as a function of welding temperature using a wedge cleavage fracture test. This allows us to indirectly examine the interpenetration behavior of incompatible interfaces via an assumed microdeformation model and compare the results to a theory developed by Helfand et al.[3,4] According to this theory the interpenetration depth as a function of temperature is related to the Flory–Huggins interaction parameter χ. A scaling argument relates the equilibrium interpenetration distance (d_∞) of the asymmetric incompatible (PS–PMMA) case with the fracture of a symmetric PS–PS sample at short welding times. Analysis of the fractured surface was conducted by using X-ray photoelectron spectroscopy (XPS) in conjunction with an optical dyeing technique to determine the type of fracture. It has been reported that fracture is adhesive[5] or a combination of adhesive and cohesive.[6]

Theoretical Considerations

The concentration profile of an incompatible polymer interface as determined by Helfand[3,4] is shown in Figure 1. Monomer units from one side diffuse to the other side until an equilibrium distribution is reached having a characteristic interpenetration depth (d_∞). The greater the amount of mixing or chain interpenetration at the interface, the greater the strength development.

The interfacial mixing of an incompatible pair of polymers is believed to depend on two counteracting forces. The first force is repulsion of chain segments in the presence of incompatible chain segments due to an interaction energy. The second force is entropic in nature and allows chains near the interface with reduced entropy, which may lie in unfavorable conformations, to increase their entropy by crossing the interface. Helfand et al.[3,4] theoretically examined the incompatible interface between two immiscible polymers of infinite molecular weight and described the diffusion of one polymer species into another by solving the diffusion equation of a random walk in a potential field due to the presence of an incompatible monomer. In particular, they determined an expression for the equilibrium interpenetration zone (d_∞) or depth of a polymer chain with respect to the Flory–Huggins interaction parameter[7] (χ)

$$d_\infty = 2b/(6\chi)^{1/2} \quad (1)$$

where b is the statistical segment step length and is taken as 6.5 Å for PS and PMMA.[3,4]

To relate the interface structure to mechanical strength, we compare the structure and strengths of the incompatible interface with the partially diffused symmetric interface. We assume that the stength that exists at d_∞ can be related to the strength that exists at a corresponding average

0024-9297/91/2224-1397$02.50/0

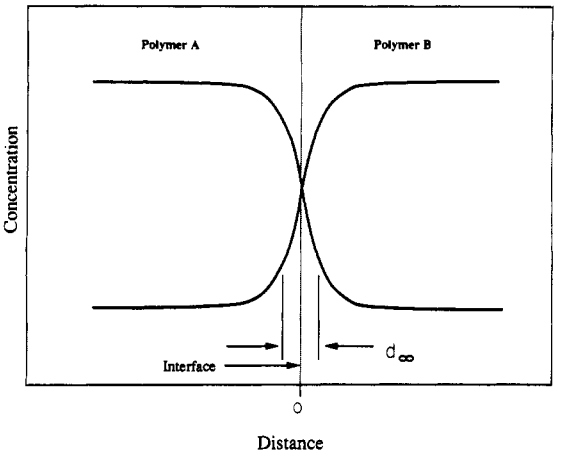

Figure 1. Concentration profile of an incompatible polymer interface as determined by Helfand.

monomer interpenetration distance $X(t)$ for the partially diffused symmetric interface. The fracture energy of the symmetric interface is given by[1,2]

$$G(t) = G_o[t/T_r]^{1/2} \quad (2)$$

where $G(t)$ is the fracture energy at time t and G_o is the maximum fracture energy attained at the reptation time, T_r.[9] This relationship assumes that chain disentanglement dominates the fracture mechanism. When chain rupture dominates, a similar equation applies, except T_r becomes the time at which the maximum strength G_o is obtained.

The average monomer interpenetration distance of the symmetric interface is given by de Gennes[9] as

$$X(t) = X_o[t/T_r]^{1/4} \quad (3)$$

where X_o is the interpenetration distance attained at T_r. X_o is related to the radius of gyration R_g by[8]

$$X_o = 0.81R_g \quad (4)$$

The strength of the interface is related to the averge interpenetration of the minor chain contour length $l(t)$ via $G(t) \sim l(t)$. Since $l(t) \sim X(t)^2$, then

$$G(t) \sim X(t)^2 \quad (5)$$

We can relate the strength of an incompatible interface in a like manner but consider only the final equilibrium positions rather than the time dependence. The average monomer interpenetration distance is thus given by X_∞ and only describes half of the interface. It is related to the equilibrium thickness, d_∞, to an excellent approximation by

$$d_\infty = 2X_\infty \quad (6)$$

Resulting in

$$G_{IC} \sim d_\infty^2 \quad (7)$$

We propose that the ratio of X_∞ (which is $(1/2)d_\infty$) to $X(t)$ is equal to the square root of G_{IC} to $G(t)$ as shown by

$$d_\infty/2X(t) = [G_{IC}/G(t)]^{1/2} \quad (8)$$

and by substitution of eqs 3 and 4

$$d_\infty = 1.62R_g[t/T_r]^{1/4}[G_{IC}/G(t)]^{1/2} \quad (9)$$

and for the special case where $t = T_r$, eq 9 reduces to

$$d_\infty = 1.62R_g[G_{IC}/G_o]^{1/2} \quad (10)$$

These equations allow one to relate the strength of the partially interpenetrated incompatible interface to the structure and strength of the partially and fully diffused interface. The utility of these equations will be discussed later.

The temperature dependence on χ can be written as[7]

$$\chi(T) = A/T + B \quad (11)$$

where A and B can be experimentally determined. By substitution into eqs 1 and 7, we find that

$$G_{IC}(T) \sim 1/(A/T + B) \quad (12)$$

For the case i where $A/T \gg B$, we find that G_{IC} varies reversibly with T as

$$G_{IC}(T) \sim T \quad (13a)$$

while for case ii where $A/T \ll B$, $G_{IC}(T)$ is independent of temperature.

$$G_{IC}(T) \sim T^0 \quad (13b)$$

These relations for G_{IC} and d_∞ will be examined in the Results section.

Experimental Section

We chose two polymers with similar moduli and glass transition temperatures (T_g). PS was obtained from The Dow Chemical Co. (Midland, MI) with a M_w of 302 000 and a polydispersity of 2.36. PMMA was obtained from Rohm and Haas Co. (Bristol, PA) with a M_w of 120 000 and a polydispersity of 1.94. The modulus for both materials was measured with a 3-point bending test and determined to be 2.7 GPa (390 000 psi). The T_g of PS was 105 °C, and the T_g for PMMA was 108 °C, determined with a Perkin-Elmer Model DSC 4 thermal analysis system at a heating rate of 20 °C/min.[6]

Preparation. The preparation of samples involved first drying the pellets in a vacuum oven at 80 ± 5 °C for 24 h. The dried pellets were molded into plaques at 160 ± 5 °C in a Carver Press (Fred S. Carver, Inc., Menomonee Falls, WI) against chrome steel mirror polished ferro plates (Apollo Metals, Inc., Bethlehem, PA) with a 12.7 cm × 12.7 cm × 0.317 cm steel mold. A 25-min warmup and a 30-min compression time were used, with a 3.5-h cool down at low pressure to minimize residual stress and orientation. Samples were observed under crosspolars and found to exhibit no birefringence. These plaques were then trimmed by 0.5 cm on each of the sides and cut into four sample sheets of 53.5 mm ± 0.5 mm square. The cutting edge burrs were removed by sanding with 320-grade carbide paper. Care was taken to protect the welding surface during the sample preparation (i.e., no contact of surfaces with metal, solvents, fingers, etc.). Polymer dust from the cutting and sanding operations was removed with freon gas microdusters. All samples were stored in a vacuum oven at 80 °C between procedures.

Welding Step. The welding process consists of placing the two incompatible sample sheets together at room temperature and quickly heating them to the desired welding temperature. The process has been designed to ensure temperature and pressure uniformity as well as reduce sample deformation above T_g. Before welding, sample sheets were removed from the vacuum oven after a minimum of 24 h and placed directly into the preheated welding block. The welding block is shown in Figure 2. It consists of aluminum pieces designed to prevent the 53-mm square polymer samples from excessively deforming (less than 3% thickness change) at temperatures above T_g and unbolts to allow removal of samples without damage to the weak interface. The welding block was placed into a preheated Carver Press to apply a vertical pressure during the welding stage as well as to provide a means of controlled heating. First, the block with samples was warmed up for 3 min from room temperature to the press temperature. Second, a pressure of 600 psi was applied and held constant with temperature (±0.5 °C) for the desired welding time. The sample temperatures of several dummy samples with temperature probes were uniform after an additional 3–4 min beyond the warm-up period. In general, the welding time was 6000 or 8000 s in order to compare with previous laboratory results.[6] The samples were

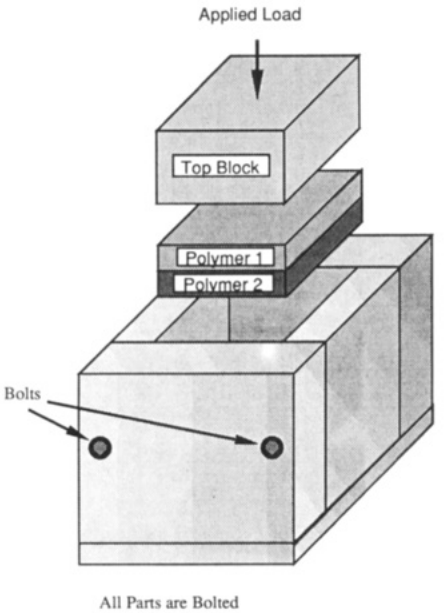

Figure 2. Diagram of the welding block.

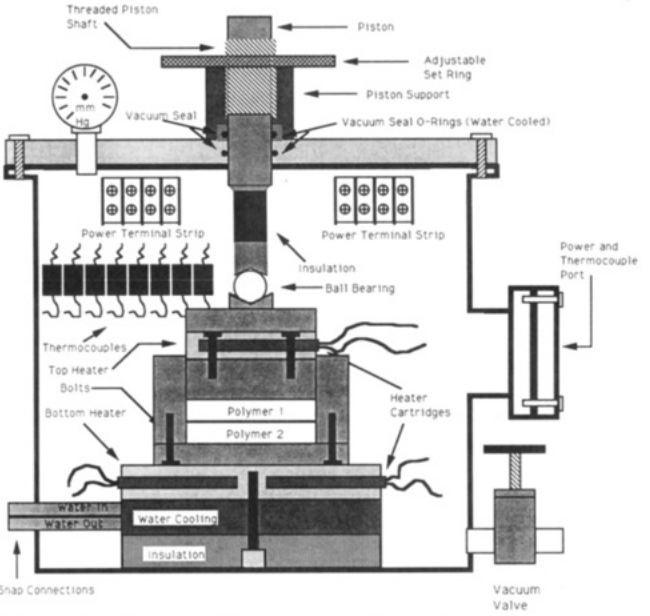

Figure 3. Diagram of a vacuum welding chamber.

then cooled from the set temperature to below 100 °C in approximately 3–5 min by removal from the press and placement on a large metal block at room temperature. None of the samples showed any indications of bubbles at the interface, which would indicate entrapped air.

An alternate procedure developed during this study was to place the welding block in a vacuum welding chamber designed specifically for this block (Figure 3). Welding under vacuum is desirable to prevent entrapped air during the wetting of the interface. The welding block was placed into the chamber with no load and a low vacuum drawn with a rotary vane vacuum pump. The sample was then heated with a top and bottom heater assembly to 95 °C and allowed to equilibrate for 5 min. The load (600 psi) was then applied via a hydraulic piston assembly and the sample allowed to heat up to the desired set temperature. The proportional controllers allowed a rapid heat up time (300 s), stable cycling (±0.2 °C), and quick reproducible settings. The results from both procedures agreed, although the reproducibility was improved with the vacuum experiments.

After welding, two opposite edges of the sample blocks were trimmed 0.4 cm with a power band saw and a fine tooth blade to remove any edge defects. The resulting piece was cut into four 9.5 mm × 53 mm samples and the cut edges polished with carbide paper (220 grade to 1000 grade). This results in a transparent sample with reduced edge defects and an enhanced capability to optically monitor the fracture and deformation process. Although this cutting and polishing step may influence the fracture strength, no correlation was observed and sample reproducibility was good as shown in the Results section. The final sample dimensions were as follows: thickness of 6.55 mm ± 0.14 mm, width of 8.66 mm ± 0.35 mm, and a length of 52.8 mm. A 10-mm crack was initiated with a razor blade, and a groove for the wedge measuring 0.76 mm thick and 2.90 mm deep was centered and cut on the top interface. These samples were also dried for a minimum of 24 h in the vacuum oven at 80 °C before testing.

XPS Analysis. Analysis of the fracture surface helps determine whether fracture is adhesive or cohesive. We expect that a fracture surface that is the result of chain disentanglement only should fail primarily due to an adhesive process. In adhesive failure, fracture occurs at the original interface while in cohesive failure fracture occurs some distance away into the weaker matrix.

X-ray photoelectron spectroscopy (XPS) was carried out with a PHI 5400 (Perkin-Elmer Corp., PE Division, Eden Prairie, MN). We used a magnesium anode and a spot size of 1.1 mm. In principle, this technique makes use of the photoelectric effect. Low-energy X-rays are used to irradiate the surface of a sample, and the kinetic energy of the ejected electron is analyzed. The kinetic energy is the difference between the photons energy and the ejected electrons binding energy from specific atoms. It is this binding energy that determines the elemental composition. Since electrons have a very small escape depth (20–50 Å), the technique is considered to be excellent for surface analysis.

In particular, we were concerned with the atomic ratios of the O_{1s} (540 eV) to C_{1s} (285 eV) ratios. If PMMA was transferred to the PS side, a strong O_{1s} signal should develop, while for the PS transfer to PMMA, a decrease in the O_{1s} signal should occur. Surface studies were conducted on both the PS and PMMA fracture surfaces of the wedge cleavage specimens (WC). Three to five spots, about 5–10 mm apart, were selected on each sample to ensure a good representation of the fracture surface. Samples were also examined in areas identified as crazed and clear fracture areas. All samples were dried 24 h at 80 °C under vacuum prior to analysis. Controls of PS and PMMA compression-molded surfaces in like manner as the WC specimens were also measured.

Optical Dye Technique. With use of a technique developed by Cho and Gent,[10] the fracture surface of the PMMA was examined by dyeing any polystyrene found on the surface. This was accomplished by using the difference in solubility properties between the two polymers. Cyclohexane is a good solvent for PS but a poor solvent for PMMA. Thus a dissolved dye penetrates any PS fragments on the PMMA fracture side and shows up as a red fracture surface on the PMMA side.

A 0.1% solution of Oil Red 4B (Pfaltz and Bauer Co.) was prepared in cyclohexane and filtered to remove large particulates. The clear red solution was applied to the fracture surfaces and allowed to dry. Care was taken to ensure that the solvent remains on the surface and does not wash off the PS. It was found that several drops of the solution would coat the entire fracture surface and that surface tension kept the solvent on the surface. After a 5-min wash in isooctane (a poor solvent for both PS and PMMA but not for the dye), the samples were air dried and examined with an optical microscope.

Fracture Experiments. A wedge cleavage (WC) geometry,[11–14] sometimes called a modified double cantilever beam (DCB), was used with a servohydraulic MTS Model 820 to measure the critical strain energy release rate, G_{IC}. This is the energy required to advance a crack on a unit area basis. As shown in Figure 4, a wedge is driven downward into the interface at 0.254 mm/min until a crack is observed to advance with a traveling microscope. For convenience, a video system is employed with the microscope to record the crack and aid in the observations. Once a crack is observed to advance, the wedge motion is stopped and the crack is allowed to advance at constant displacement until the stress at the crack tip is reduced enough to prevent further cracking. In practice, most of the growth process is completed after 15 min. Although, the crack will continue growing slowly even after several hours probably due to a polymer chain creep relaxation phenomena. The displacement (m) was mea-

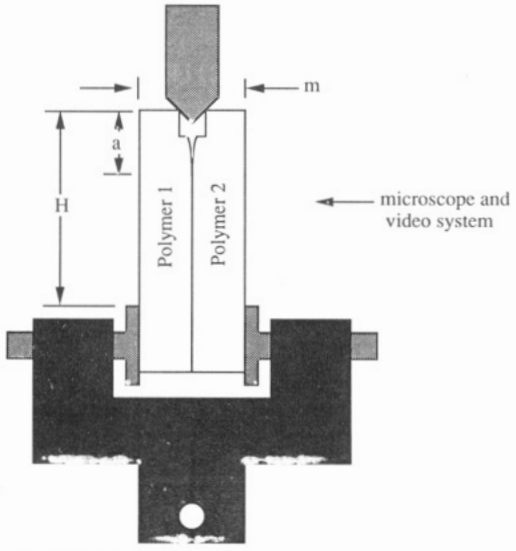

Figure 4. Wedge cleavage experiment.

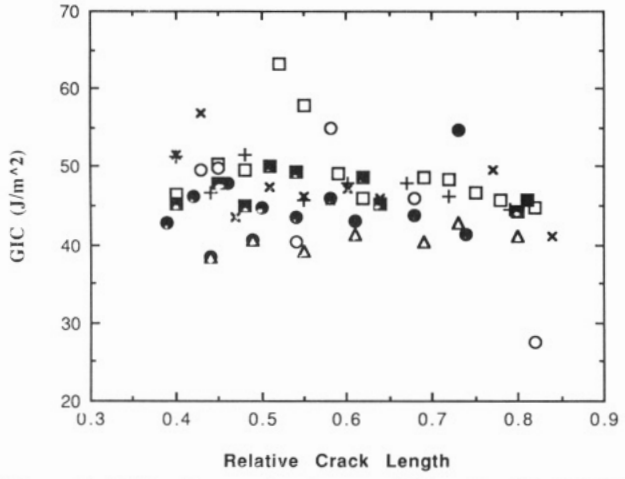

Figure 5. Wedge cleavage fracture results from two PS–PMMA interfaces.

sured to ±0.01 mm, the sample removed, and the crack length (a) measured to ±0.1 mm. This procedure was repeated as many as 15 times per sample, resulting in approximately 40 measurements per welding experiment. In practice, we have chosen to use the G_{IC} arrest over the true critical strain initiation value, as it is constant with the arrested crack length along the length of the sample. The length of the sample outside the grips is slightly different for each sample. In order to better compare one sample to another, we defined a relative crack length as the ratio of the arrested crack length to the length of the specimen outside the grips (H) as shown in Figure 4.

Kanninen[15] derived an expression for G_{IC} with a double cantilever beam geometry on an elastic foundation and obtained the result

$$G_{IC} = \left(\frac{3}{16}\right)\frac{(m-2h)^2Eh^3}{a^4}\left[1 + 0.64\left(\frac{h}{a}\right)\right]^{-4} \qquad (14)$$

where m = separation of the outside top surface of the sample (displacement), $2h$ = total sample thickness, E = Young's elastic modulus, and a = crack length.

Thus, the displacement ($m - 2h$) due to the wedge and crack length a are measured and used in eq 14 to analyze G_{IC}.

Results

Fracture Energy of a PS–PMMA Interface. Wedge cleavage fracture results from two PS–PMMA interfaces are shown in Figure 5. Here, G_{IC} is plotted as a function of the relative crack length (a/H). These results show the

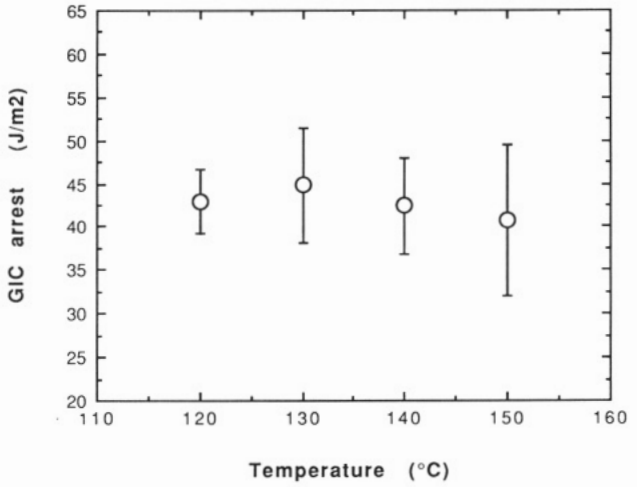

Figure 6. G_{IC} of a series of PS–PMMA samples welded at four different temperatures between 120 and 150 °C.

experimental reproducibility between samples prepared, welded, and cut under similar conditions. These samples were obtained from two welding experiments at 140 °C for 6000 s and show typical sample reproducibility. Four of the samples were from one welding block while the other three were from a different block. The data show good reproducibility with a standard deviation within 10–15% of the measured value both along the crack length of the sample and in comparison to neighboring samples from the same welding sheet as well as from block to block. This indicates uniform if not complete wetting and shows expected scatter from a fracture experiment. More importantly, the G_{IC} arrest values were determined to be independent of the relative crack length, supporting the use of eq 14 for these experiments. Sample scatter is the result of many conditions typical in fracture experiments including sample preparation and the measurement of displacement (m), as well as vibrations of the hydraulic unit acting on the weak interface. The average G_{IC} value is 45.5 ± 4.1 J/m^2.

Samples were also measured for welding times of 600 s and gave similar average fracture results, although the scatter in the data was generally increased. Here, the average strength was 42.7 ± 4.86 J/m^2 for samples welded at 140 °C for 600 s. A summary of results is given in Table II.

These values are significantly lower than the virgin values (G^*) for either the PS or PMMA. G^* has been measured with a variety of fracture geometries,[12,13,16,17] and its value is dependent upon molecular weight up to some critical molecular weight.[2] For PS this critical molecular weight is 100 000–250 000 depending on the fracture test.[2,17] At higher rates generally used with the Charpy impact and compact tension geometries, the strength at and above the critical molecular weight is approximately 600–1000 J/m^2. Our results are also much higher than predicted by the Griffith theory of fracture.[16,18] where the G_{IC} is equal to 2 times the surface energy ($\Gamma_{PS} \simeq 0.04$ J/m^2).[12] This demonstrates that the fracture energy of polymers is dominated by deformation mechanisms other than the energy required to create a new surface.

Temperature Dependence of G_{IC}. We measured the G_{IC} of a series of PS–PMMA samples (Figure 6) welded at four different temperatures between 120 and 150 °C and found it independent of temperature with an average of 42.5 ± 4.5 J/m^2. This supports case ii of eq 13 whose χ is largely independent in this range. Furthermore, by comparing G_{IC} at two different temperatures, we can

predict the difference in χ at the same temperature range (T_1,T_2) from

$$G_{T_1}/G_{T_2} = \chi_{T_2}/\chi_{T_1} \quad (15)$$

From our results above we would then predict little or no change in χ. In fact χ has been recently measured for a PS–PMMA diblock system as a function of temperature within this temperature range by Russel et al.[19] and behaves as

$$\chi = 0.0284 + 3.902/T \quad (16)$$

where T is the temperature in degrees Kelvin. The interaction parameter, χ, only changes by 0.1% for the temperature range of 120–150 °C. This change agrees well within our experimental value of $G_{IC} = 42.5 \pm 4.5$ J/m^2. This temperature independence of G_{IC} contrasts with a slight temperature dependence reported by Willett[6] but agrees with the magnitude of G_{IC} in this temperature range.

Comparison to Previous Studies. As stated previously, these results are in slight contrast with an earlier study by Willett. There are several differences in the preparation of these samples and in the analysis of the data that may account for these differences.

The thermal history of both methods is substantially different. The procedure described by Willett used welding plates wetted at 140 °C for 120–300 s and then cooled down to room temperature. The plates were cut into free samples. These samples were measured to determine a "zero" time fracture strength and placed back into an oven for a specific welding time at the test temperature (ranging from 112 to 142 °C). The fracture strength was determined and the procedure repeated for as many as four heating and cooling cycles to obtain the fracture strength as a function of welding time.

The thermodynamic nature of the interface and how it behaves during the cooling stage of a welding experiment are of some concern. Interfacial demixing upon cooling may occur, thus leading to a decrease in strength. The thermal shock and mismatches in coefficient of expansions might lead to failures at the interface. When the temperature is cycled between the fracture measurements, another uncertainty is produced and may lead to misleading results. To reduce this effect, we chose to examine the specimens under a one-step wetting/welding stage that was always at the test temperature.

Samples were subsequently stored at 70–80 °C in a vacuum oven before testing to reduce effects of moisture at the interface. We were concerned with strength stability during these long annealing times, as some motion of the molecule at the interface could be expected even at temperatures below T_g. The longest time a sample was in the oven was 7 days, and the shortest was 1 day. No differences were observed in the fracture strength as a result of this thermal history.

The statistical sampling and treatment of the data is also a point of difference between the two studies. It is difficult to determine how many data points are involved with the previous study,[6] and it is possible that the temperature effects are the result of only four samples of which only a portion of each was used. Significant sampling is crucial in fracture mechanic experiments. Under the best of conditions, one-step welding and comparing samples from the same welding block, we find that the average strength of a sample will vary by 5 J/m^2 and the scatter in the data from all four samples will be in a range of 10–15 J/m^2 about the average (Figure 5). The strength difference observed by the previous study was approximately 10–12 J/m^2 for temperatures between 120 and 140 °C, which agrees well with the standard deviation observed in this study for the same temperature range. The magnitudes of the results in our study are slightly higher than those in the previous study.

Table I
Fracture Strength of Virgin Polystyrene

technique	mol wt	fracture strength, J/m^2	calcd[a] d_∞
compact tension	250 000	1000[2]	46
compact tension	100 000	200[2]	65
charpy impact	100 000	1000[17]	29
wedge cleavage	111 000	98[12]	99

[a] d_∞ determined from eq 6 of text.

The last effect is the pressure at which the samples were wetted or welded. Our study used significantly higher pressures to ensure complete wetting of the interface. This should lead to more reproducible data from sample to sample.[2] The welding block allowed the higher pressures by containing the sample as well as providing more uniform heating. This method was not available at the time of the previous study.

Interface Thickness. The interpenetration depth can be calculated as a function of temperature by substituting eq 16 into eq 1. We find this depth for a temperature range of 120–150 °C to vary from 27.1 to 27.4 Å. Fernandez and Higgins[20] report, on the basis of neutron reflection experiments, that the interfacial thickness of a PS and PMMA sample heated for 6 h at 120 °C was determined not to be greater than 20 ± 5 Å. However, Russel et al., also using neutron reflection, obtained a d_∞ of approximately 50 Å for this temperature range.[21]

As shown earlier, we can relate the PS–PMMA fracture results with the virgin PS fracture results and calculate a d_∞ with eq 10. By substituting the fracture strength of virgin PS, measured with compact tension,[2] of 1000 J/m^2 at a number-average molecular weight (M_n) of 250 000, we find d_∞ to be 46 Å. At a lower M_n of 100 000, the fracture strength was measured to be near 200 J/m^2, with a d_∞ = 65 Å.

One must be cautious in comparing fracture results based on different rates, geometries, molecular weights, and polydispersities. Table I summarizes various d_∞ values calculated based on fracture strengths reported in the literature for different molecular weight PS using a variety of techniques. When results reported by Greco[17] are used with a M_n of 100 000 and a fracture strength of 1000 J/m^2, d_∞ is calculated to be 29 Å. Robertson[12] reports much lower fracture results using a wedge cleavage geometry. For a PS sample with a M_n of 111 000, he measured a range of G_{IC} from 27.4 to 166 J/m^2, with the average being 98 J/m^2. This results in a calculated d_∞ of 99 Å.

To avoid the problems of comparing fracture strengths determined with various experimental geometries with our WC results, we have measured the strength of a PS–PS interface at short welding times. Because it is difficult to measure the strength of the virgin material using the WC technique, we have chosen to measure the strength when only a small portion of the polymer chain has crossed the interface. This should more closely resemble the fracture that occurs for an incompatible case and is probably more valid for Wool's[1] chain pull out arguments than a high molecular weight virgin material.

This interpenetration distance can be determined from eq 9 by substituting eq 17 where M_n is the molecular weight

$$R_g = \left[\frac{M_n(2C_\infty)}{6M_o}\right]^{1/2} b \quad (17)$$

Table II

temp, °C	welding time, s	G_{IC}(av), J/m²	stand deviatn, J/m²	sample[a]
120	800	41.7	3.91	A1
120	800	45.2	4.64	A2
120	6000	39.4	3.10	B1
120	6000	45.4	3.23	B2
130	8000	48.5	3.50	C1
130	8000	49.4	3.70	C2
130	8000	37.4	3.80	D1
140	600	37.2	2.70	E1
140	600	45.3	4.20	E2
140	600	43.9	2.70	E3
140	6000	50.3	6.09	F1
140	6000	46.7	6.70	F2
140	6000	47.2	2.17	F3
140	6000	45.2	3.16	F4
140	8000	48.4	3.50	G1
140	8000	36.8	8.30	G2
140	8000	43.9	4.50	G2
140	8000	36.9	2.90	H1
140	8000	40.0	4.00	H2
140	8000	34.8	8.10	H3
140	8000	40.3	4.60	H4
140	8000	33.8	10.10	I4
150	8000	28.4	8.50	J1
150	8000	29.9	8.70	J2
150	8000	31.2	10.60	J3
150	8000	59.3	10.00	K1
150	8000	54.6	5.82	K2

[a] The letter indicates the block, and the number represents the sample of each block; i.e., H1 and H2 are samples 1 and 2 from block H.

of the polymer chain, M_o is the weight of one monomer unit (105), C_∞ is the characteristic ratio (10), and b is the monomer segment length (1.54 Å), resulting in

$$d_\infty = 0.45(M_n)^{0.5}\left(\frac{t}{T_{rep}}\right)^{1/4}\left[\frac{G_{IC}}{G(t)}\right]^{1/2} \text{(Å)} \qquad (18)$$

Experimental wedge cleavage results were obtained for a PS–PS sample that was welded for 21.5 ± 3 min at 115 ± 1 °C. With M_n = 128 000 the calculated reptation time was 516 min at 115 °C and $G(t$=516 min) = 54 ± 10 J/m². By use of the previously measured value of G_{IC} for PS–PMMA (42.5 J/m²), d_∞ determined for the PS–PMMA interface is 60 ± 20 Å. The 20-Å deviation represents a combination of experimental error in welding time, temperature, and fracture strength.

Observations and Analysis of Fracture Surfaces. In general, two distinct types of fracture were observed with these samples, often on the same sample. The first and more common was a visible crazing, which clouded the interface and resulted in a rough fracture surface on both sides of the specimen. This type of fracture will be called crazed fracture. Observations of the PS and PMMA fracture surfaces with an optical microscope appeared very similar. As previously observed by Willett[6] using SEM, ridges are observed on the PS side which run perpendicular to the crack growth. We also observe ridges on the PMMA side to a greater extent than described by Willett. Willett interpreted these ridges on the PS side as PS regions drawn during fracture and the ridges on the PMMA side also as PS but due to a cohesive fracture. His XPS results supported this, as he determined no PMMA on the PS surface and did detect PS on the PMMA side. He concluded that there was a mixture of adhesive and cohesive fracture that contributed to his strength measured.

In contrast to these observations are fracture regions of a second type not reported by Willett. Here fracture is rapid with little deformation on either side of the interface. We will call this fracture clear fracture. These surfaces could easily be interpreted as adhesive failure, but XPS results presented below do not agree. Samples from the same welding block that were adjacent to each other during the welding process did not have crazed and clear regions in common, indicating that these regions were not due to wetting problems. Oddly enough, the measured fracture energy results did not depend on the type of fracture observed.

The cracks were recorded with a video camera and traveling microscope system to replay the process of the crack growth. Here we observed that the crack travels not as one single front but as a multitude of minor fronts coalescing together. These fronts do converge from time to time and travel with a common front speed, which varied from measurement to measurement. In any one measurement the velocities of these minor fronts are not constant but occur as small steps, much like the stick slip descriptions.[6,12]

Measurements were made with XPS on PS and PMMA fracture surfaces. As did Willett,[23] we found that the oxygen content at the PS fracture surfaces was at or below trace levels, indicating that no PMMA was on the PS fracture surface. The PMMA fracture surface was also examined and found to have a small but significant decrease in oxygen to carbon ratios, indicating failure was at least partially cohesive. The O/C ratio of a PMMA control sample was found to be 0.365 ± 0.064, which is close to the theoretical result of 0.40 (two oxygens to five carbons). The PMMA fracture surfaces of a PS–PMMA sample were found to have an average of 0.250 ± 0.026 ratio. These results were obtained regardless of whether the measurement was made on a fracture surface with crazed regions or on the clear fracture zones and indicates that some PS is transferred regardless of the type of fracture. On a unit volume basis, this results in an approximate 30% coverage with PS or possibly a thin 10–20-Å PS coating on the PMMA surface. All XPS results were in good agreement with past results in our own lab by Willett.[6]

The analysis of the fracture surface is quite complicated, and its relation to the strength can be debated. We saw equivalent strength in a series of clearly different fracture regions (i.e., crazed and clear). This leads to a conclusion that G_{IC} values measured with this technique are the result of more than just the strength of the interface.

In both types of fracture, the edges of the polystyrene side of the samples, near the crack tip, had crazes growing perpendicularly to the interface plane into the PS side. The largest craze observed was 0.5 mm long, but most were much smaller. These crazes were not observed ahead of the crack tip and may be due in part to the beam bending of the PS leading to a tension stress component at the interface. The occurrence of this crazing only on the PS side is most likely due to its lower craze stress in comparison to PMMA.[24] Brown[5] also observed this and developed an asymmetric cleavage test to suppress tendency of crazes to grow away from PS–PMMA interfaces into the PS side, resulting in larger toughness values. He found by bonding the PS to a rigid substrate that G_{IC} values were 5–10 J/m² in comparison to a free-standing result of 60–100 J/m². By bonding the PMMA to a rigid surface, values near the strength of PS were observed.

When the fracture surfaces were first observed with an optical dye technique very little PS was observed on the PMMA surface. In this experiment, the PS shows up as red areas due to the solubility difference of PS and PMMA in cyclohexane. In the typical crazed regions some red

spots were observed but not on all of the fracture surface. In fact less than 1% of the surface stained red, indicating very little PS on the PMMA surface. On the fracture surface with less surface damage, almost no PS could be detected. This was also observed by Cho and Gent[10] for a series of torsion-fractured specimens of PS welded to PMMA.

It is possible that the dyed PS thickness is so small that the intensity of color is below the detection threshold. By an increase of the dye concentration by almost 2 orders of magnitude to 9%, it became clear that there was greater coverage on the crazed zones than first observed. Although the contrast is too slight to publish photographs, we can observe small "pools" of red tint on the PMMA fracture surface matching closely with the previously described PS ridges. The coverage is approximately 5–20%. The clear fracture zones did not indicate any greater coverage than before. Perhaps there is PS on these surfaces as well but below detection limits. XPS analysis is far more sensitive to a thin layer of PS on the surface than the optical dye.

Summary and Conclusions

The fracture strength of polystyrene and poly(methyl methacrylate) interfaces is independent of welding temperature over a range of 120–150 °C. We found an average strength of 42.5 ± 4.5 J/m^2 for these incompatible polymers, which is both significantly lower than the fracture strength of virgin polystyrene and higher than the surface energy of the polymer. If fracture strength is inversely proportional to the Flory–Huggins interaction parameter (χ), then χ is largely independent of temperature. This result is supported by Russel's experimental determination that χ is independent of temperature in the range 120–150 °C.

By use of a reptation minor chain model, calculations of the interpenetration depth (d_∞) with virgin and short-time welding data of symmetric interfaces yield a value with the same order of magnitude as measured values determined with neutron reflection experiments by Higgins et al.[20] and Russel et al.[21] We calculate 60 ± 20 Å for short-time welding in comparison to Higgin's 25-Å result and Russel's 50-Å result. These results are also in agreement with the order of magnitude of Helfand's theory of d_∞ = 27 Å but are a little higher.

On the basis of the surface analysis, we conclude that there is probably a combination of adhesive and cohesive failure and that the cohesive failure occurs very close to the interface on the PS side only. This is probably due to the lower craze stress of PS in comparison to PMMA. A surface analysis with XPS determined that some PS was transferred to the PMMA side as a result of the fracture, indicating some cohesive fracture, but no PMMA was transferred to the PS side. These results occurred regardless of the type of fracture surface (i.e., crazed or clear fracture zones). An optical dye study found some evidence of polystyrene transferred onto the fracture surface of PMMA with less than 20% coverage of crazed fracture zones testing positive for PS and no PS observed on the clear fracture zones. This may be due to intensity detection limits.

Acknowledgment. This project was supported by IBM, The Dow Chemical Co., and the Army Research Office, Grant DAAL 03-86-K-0034. The XPS experiments were completed at the Center of Microanalysis of Materials, University of Illinois, which is supported by the U.S. Department of Energy under Contract DE-AC 02-76ER 01198.

References and Notes

(1) Kim, Y. H.; Wool, R. P. *Macromolecules* **1983**, *16*, 1115.
(2) Wool, R. P.; Yuan, B.; McGarel, O. *J. Polym. Eng. Sci.* **1989**, *29*, 1340.
(3) Helfand, E.; Tagami, Y. *J. Chem. Phys.* **1971**, *56*, 3592.
(4) Helfand, E.; Sapse, A. M. *J. Chem. Phys.* **1975**, *62*, 1327.
(5) Brown, H. R. To be published.
(6) Willett, J. L. Ph.D. Thesis, Department of Mining and Metallurgy, University of Illinois, Urbana, IL, 1987.
(7) Flory, P. J. *Principles of Polymer Chemistry*; Cornell University Press: Ithaca, NY, 1983.
(8) Zhang, H.; Wool, R. P. *Macromolecules* **1989**, *22*, 3018.
(9) de Gennes, P.-G. *J. Phys. (Fr.)* **1989**, *50*, 2551.
(10) Cho, K.; Gent, A. N. *J. Adhes.* **1988**, *25*, 109.
(11) Berry, J. P. *J. Appl. Phys.* **1963**, *34*, 62.
(12) Robertson, R. E. *Toughness and Brittleness of Plastics*; Deanin, Crugnola, Eds.; Advances in Chemistry Series 154; American Chemical Society: Washington, DC, 1976.
(13) Broutman, L. J.; McGarry, F. J. *J. Appl. Polym. Sci.* **1965**, *9*, 589.
(14) Broek, D. *Elementary Engineering Fracture Mechanics*; Martinus Nijhoff Publishers: Dordrecht, The Netherlands, 1982.
(15) Kanninen, M. F. *Int. J. Fract.* **1973**, *9*, 83.
(16) Broutman, L. J.; McGarry, F. J. *J. Appl. Polym. Sci.* **1965**, *9*, 609.
(17) Greco, R.; Ragosta, G. *Plast. Rubber Process. Appl.* **1987**, *7*, 163.
(18) Griffith, A. A. *Philos. Trans. R. Soc.* **1920**, *A221*, 163.
(19) Russel, T. P.; Hjelm, R.; Seeger, P. *Bull. Am. Phys. Soc.* 1989, Spring G26, 10.
(20) Fernandez, M. L.; Higgins, J. S.; Penfold, J.; Ward, R. C.; Shackleton, C.; Walsh, D. J. *Polymer* **1988**, *29*, 1923.
(21) Russel, T., private communication, IBM, July 1988.
(22) de Gennes, P.-G. *J. Chem. Phys.* **1971**, *55*, 572.
(23) Willett, J. L.; Wool, R. P. Submitted for publication.
(24) Williams, A. G. *Fracture Mechanics of Polymers*; Ellis Horwood Limited: England, 1984.

Registry No. PS, 9003-53-6; PMMA, 9011-14-7.